



**HAL**  
open science

## Effect of nonenzymatic deamidation on the structure stability of *Camelus dromedarius* $\alpha$ -lactalbumin

Saliha Si Ahmed Zennia, Abderrahmane Mati, Christophe Charron, Céline Cakir-Kiefer, Alexandre Kriznik, Jean-Michel Girardet

### ► To cite this version:

Saliha Si Ahmed Zennia, Abderrahmane Mati, Christophe Charron, Céline Cakir-Kiefer, Alexandre Kriznik, et al.. Effect of nonenzymatic deamidation on the structure stability of *Camelus dromedarius*  $\alpha$ -lactalbumin. *Food Chemistry*, 2019, 291, pp.207-213. 10.1016/j.foodchem.2019.04.033 . hal-02095313

HAL Id: hal-02095313

<https://hal.univ-lorraine.fr/hal-02095313v1>

Submitted on 22 Oct 2021

**HAL** is a multi-disciplinary open access archive for the deposit and dissemination of scientific research documents, whether they are published or not. The documents may come from teaching and research institutions in France or abroad, or from public or private research centers.

L'archive ouverte pluridisciplinaire **HAL**, est destinée au dépôt et à la diffusion de documents scientifiques de niveau recherche, publiés ou non, émanant des établissements d'enseignement et de recherche français ou étrangers, des laboratoires publics ou privés.



Distributed under a Creative Commons Attribution - NonCommercial 4.0 International License

1 **Effect of nonenzymatic deamidation on the structure stability of *Camelus***  
2 ***dromedarius*  $\alpha$ -lactalbumin**

3

4 Saliha Si Ahmed Zennia<sup>a</sup>, Abderrahmane Mati<sup>a</sup>, Christophe Charron<sup>b</sup>, Céline Cakir-Kiefer<sup>c</sup>,  
5 Alexandre Kriznik<sup>b</sup>, Jean-Michel Girardet<sup>c\*</sup>

6

7 <sup>a</sup>*Université Mouloud Mammeri, Laboratoire de Recherche de Biochimie Analytique et Biotechnologies (LABAB), Tizi*  
8 *Ouzou, Algérie*

9 <sup>b</sup>*Université de Lorraine, CNRS, Ingénierie Moléculaire et Physiopathologie Articulaire (IMoPA), UMR 7365, Nancy F-*  
10 *54000, France*

11 <sup>c</sup>*Université de Lorraine, INRA, Unité de Recherche Animal et Fonctionnalités des Produits Animaux (UR AFPA), USC*  
12 *340, Nancy, F-54000, France*

13

14 \* Corresponding author present address: Université de Lorraine, INRA, Interactions Arbres-Microorganismes (IAM),  
15 UMR 1136, F-54000 Nancy, France.

16 *E-mail address:* [jean-michel.girardet@univ-lorraine.fr](mailto:jean-michel.girardet@univ-lorraine.fr) (J.-M. Girardet).

17

18 *Keywords:* Camel  $\alpha$ -lactalbumin, Circular dichroism, Differential scanning calorimetry, Nonenzymatic deamidation,  
19 Thermolysin, X-ray crystallography

20

21 **ABSTRACT**

22 Camelid  $\alpha$ -lactalbumin is the only known protein that can undergo nonenzymatic deamidation on  
23 two Asn residues. This leads to the generation of a mixture of unusual iso-Asp and D-Asp residues  
24 that may impact health. The effect of deamidation on camel  $\alpha$ -lactalbum instability was investigated.  
25 Circular dichroism showed that the altered protein acquired secondary structure resulting in an  
26 increase in  $\alpha$ -helix content. In good agreement, the 3D structure of camel  $\alpha$ -lactalbumin determined

27 by X-ray crystallography, displayed a short additional  $\alpha$ -helix probably induced by deamidation,  
28 compared to the human and bovine counterparts. This  $\alpha$ -helix was located in the C-terminal region  
29 and included residues 101 to 106. Differential scanning calorimetry together with the susceptibility  
30 to thermolysin showed that the deamidation process reinforced the structural stability of the  $\alpha$ -  
31 lactalbumin at high temperature and its resistance toward proteolysis.

32

33 *Abbreviations:*  $\alpha$ -La:  $\alpha$ -lactalbumin; CD: circular dichroism; DSC, differential scanning calorimetry; FPLC, fast protein  
34 liquid chromatography; HAMLET, human  $\alpha$ -lactalbumin made lethal to tumor cells; HPLC, high-performance liquid  
35 chromatography; PAGE, polyacrylamide gel electrophoresis.

36

## 37 **1. Introduction**

38

39 Nonenzymatic deamidation of proteins has been studied extensively *in vivo* and *in vitro*  
40 because of its important biological effects on enzymatic activity, folding, and proteolytic  
41 degradation, and also because of its crucial role as a molecular clock *in vivo* (Aswad, Paranandi &  
42 Schurter, 2000; Robinson & Robinson, 2004). The side chain of Asn residues is prone to deamidate  
43 under physiological conditions (i.e. near-neutral or slightly basic pH and 37 °C), especially when the  
44 adjacent residue at the C-terminal side is Gly. However, ordered secondary structures such as  $\alpha$ -  
45 helices and  $\beta$ -sheets inhibit the process, as the peptide backbone and the side chains are stabilized by  
46 numerous hydrogen bonds (Robinson & Robinson, 2004). This post-translational modification leads  
47 to the production of a mixture of L-isoAsp, L-Asp, D-isoAsp, and D-Asp residues in the polypeptide  
48 chain (Aswad et al., 2000).

49 Intriguingly, a few dietary proteins, especially from milk of some species, are readily subject  
50 to nonenzymatic deamidation at the level of their Asn-Gly sequences: women's milk lactoferrin  
51 (Belizy et al., 2001), equine  $\alpha$ -lactalbumin ( $\alpha$ -La; Girardet et al., 2004) and  $\beta$ -casein (Girardet,  
52 Miclo, Florent, Mollé, & Gaillard, 2006), canine milk lysozyme (Nonaka et al., 2008), bovine  $\beta$ -

53 lactoglobulin B (Meltretter, Wüst, & Pisc, 2013), and more recently in our previous work, we have  
54 identified two deamidated isoforms of *camelus dromedarius*  $\alpha$ -La by Fourier transform ion cyclotron  
55 resonance mass spectrometry and shown that Asn<sup>45</sup> is deamidated spontaneously at pH 7.4 and 37  
56 °C, whereas Asn<sup>16</sup> needs a more basic pH higher than 8.0 to undergo a deamidation process (Si  
57 Ahmed Zennia et al., 2015). Among the investigated  $\alpha$ -Lacs, that of the *Camelidae* family (camel,  
58 guanaco, and llama) has the particularity to be the only known  $\alpha$ -La with two Asn-Gly motifs at  
59 positions 16–17 and 45–46. However, whatever the species studied, the biological significance of  
60 nonenzymatic deamidation of dietary proteins remains unknown. Si Ahmed Zennia et al. (2015)  
61 assumed that the formation of isoAsp in the gut after camel milk-derived food intake might elicit  
62 auto-immunity (Aswad et al., 2000) and might be responsible of IgE-mediated allergy as reported by  
63 Gall, Kalveram, Sick, and Sterry (1996) after equine milk consumption.

64 The  $\alpha$ -La protein is a subunit of the lactose synthase complex that promotes the synthesis of  
65 lactose in the mammary gland in response to prolactin (Kuhn, Carrick, & Wilde, 1980). It contains  
66 123 amino acid residues and its compact, globular structure is stabilized by four disulfide bonds and  
67 by the presence of a calcium ion (holo form). The globular structure of  $\alpha$ -La is composed of a large  
68  $\alpha$ -domain (regions 1–34 and 86–123) containing three  $\alpha$ -helices and two  $3_{10}$  helices, and a small  $\beta$ -  
69 domain (region 35–85) containing a three-stranded antiparallel  $\beta$ -sheet and a  $3_{10}$  helix (Chandra,  
70 Brew, & Acharya, 1998; Chrysinina, Brew, & Acharya, 2000). Besides, the 99–114 region forms a  
71 flexible loop located between  $\alpha$ -helix  $\alpha_3$  (region 86–98) and the  $3_{10}$  helix h2 (region 115–118). The  
72 calcium-binding loop including Asp<sup>82</sup>, Asp<sup>87</sup>, and Asp<sup>88</sup> is located at the junction of the  $\alpha$ - and  $\beta$ -  
73 domains and this explains why the presence of one calcium ion strongly stabilizes the protein  
74 (Chrysinina et al., 2000). Calcium binding confers a relative resistance to enzyme proteolysis and  
75 different strategies to remove calcium are being developed to increase the susceptibility of  $\alpha$ -La  
76 towards proteases, such as acidification (Schmidt & Poll, 1991), heat treatment (N'Negue et al.,  
77 2006), or zinc ion binding (Permyakov & Berliner, 2000). In the absence of calcium (apo form), the  
78 protein adopts a molten globule state sensitive to proteolysis. The molten globule is defined by a

79 partly unfolded, reversible structure for which the 3D structure is poorly defined whereas the  
80 secondary structure remains unchanged (for review see Ptitsyn, 1995).

81 The  $\alpha$ -La protein displays many biological properties. In human, apo- $\alpha$ -La, in molten globule  
82 state, can form a complex with oleic acid (C18:1  $\omega$ 9-*cis*), thus acquiring a tumoricidal activity  
83 against cancer cells of different origin. This complex is known as HAMLET (for human  $\alpha$ -  
84 lactalbumin made lethal to tumor cells; Ho, Nadeem, & Svanborg, 2017). Similarly, camel  $\alpha$ -La is  
85 able to bind oleic acid and acquires cytotoxic effect vs. human prostate cancer cells (Atri et al., 2011)  
86 or breast cancer cells (Uversky, El-Fakharany, Abu-Serie, Almehdar, & Redwan, 2017). In cow's  
87 milk,  $\alpha$ -La is considered as the least allergenic milk protein (Natale et al., 2004), contrary to  $\beta$ -  
88 lactoglobulin, which is the most abundant soluble protein and one of the major milk allergens  
89 responsible for cow milk allergy (Wu et al., 2018). The camel milk has the particularity to be free of  
90  $\beta$ -lactoglobulin and therefore,  $\alpha$ -La is the most abundant among the soluble proteins (higher than 5  
91 g/L, Alavi, Salami, Emam-Djomeh, & Mohammadian, 2017). Another advantage of camel  $\alpha$ -La is  
92 its antioxidant power, more efficient than that of bovine  $\alpha$ -La (Salami et al., 2009). Besides, the  
93 camel  $\alpha$ -La possesses a nutritional interest, as it contains a high concentration of essential amino  
94 acids in agreement with its polypeptide sequence (Swiss-Prot accession number P00710), slightly  
95 higher than the bovine counterpart, as noticed by Salami et al. (2009).

96 The degree of hydrolysis obtained by trypsin (E.C. 3.4.21.4) or chymotrypsin (EC 3.4.21.2)  
97 treatment is higher with camel  $\alpha$ -La than with bovine  $\alpha$ -La (Salami et al., 2009). This is explained  
98 by conformational and structural differences between the two homologous proteins, as shown by  
99 fluorescence measurements performed by Salami et al. (2009). Despite the attractive nutritional  
100 value of  $\alpha$ -La, low digestibility is reported for this protein, especially in the stomach the pH of which  
101 is 5–6 during a milk intake, preventing the action of pepsin (E.C. 3.4.23.1) which has an optimal  
102 activity at ca. pH 1–2 (Lindberg, Engberg, Sjöberg, & Lönnerdal, 1998). According to Salami et al.

103 (2009), in the gut trypsin and chymotrypsin play a critical role to digest  $\alpha$ -La, the camel protein  
104 appearing more sensitive than the bovine counterpart.

105 More generally, interest for camel milk use in human nutrition has increased during the last  
106 decade, as evidenced by many review-articles that report nutraceutical potential and health benefits  
107 of this milk. For instance, camel milk is used for therapeutic properties efficient against diabetes and  
108 cancer as well as for anti-hypertensive and anti-oxidative properties (for recent review, see Sakandar  
109 et al., 2018).

110 The present work focuses on *in vitro* studies of the structural stability of the main camel whey  
111 protein, namely  $\alpha$ -La, susceptible to undergo a deamidation phenomenon, especially in the gut after  
112 a milk intake. This nonenzymatic deamidation, not observed for the bovine protein, might change the  
113 stability of camel  $\alpha$ -La and have an incidence on the bioavailability in the gastrointestinal tract and  
114 thus on its biological activity and nutritional properties. The investigations were performed by using  
115 circular dichroism and X-ray crystallography, as well as differential scanning calorimetry and finally  
116 studies concerning susceptibility to proteolysis.

117

## 118 **2. Materials and methods**

### 119 *2.1. Materials*

120

121 The ÄKTA-Purifier system and the Superdex 75 column were from GE Healthcare (Uppsala,  
122 Sweden), the Amicon™ concentration cell was purchased from Merck Millipore (Darmstadt,  
123 Germany), the spectropolarimeter CD6 was from Jobin-Yvon (Palaiseau, France) and the X8-  
124 Proteum diffractometer was from Bruker AXS (Madison, WI, USA). The Microcal VP-DSC device  
125 was purchased by Malvern Instruments, Malvern, UK). The Alliance 2690 unit was from Waters  
126 (Milford, MA, USA) and the LichroCart C<sub>18</sub> column (250 x 4 mm, 5  $\mu$ m particle size, 10 nm  
127 porosity) was from Merck (Darmstadt, Germany). All the chemicals, reagents and enzymes were  
128 purchased from Sigma Chemical Co. (St. Louis, MO, USA).

129

## 130 2.2. Nonenzymatic deamidation of $\alpha$ -La and purification of isoforms

131

132 Raw milk was obtained from a herd of Sahraoui female dromedaries (*Camelus dromedarius*)  
133 and immediately stored at -20 °C until use. The pH of the fresh milk sample was 6.7. After skimming  
134 the milk by centrifugation (3500 g at 32 °C for 30 min), the casein fraction was discarded by  
135 precipitation at pH 4.3 with 1 M HCl and centrifugation. The supernatant was neutralized with 1 M  
136 NaOH, dialyzed against ultra-pure water at 4 °C for 72 h and the soluble protein fraction was freeze-  
137 dried.

138 The soluble protein fraction was dissolved at 15 mg/mL in 150 mM sodium phosphate buffer,  
139 pH 8.4 (in the presence of 0.02% sodium azide as preservative), filtered at 45  $\mu$ m, and incubated at  
140 37 °C for 96 h. After incubation, the mono-deamidated (A<sub>2</sub>) and di-deamidated forms (A<sub>3</sub>) were  
141 purified from the soluble protein fraction by anion-exchange fast protein liquid chromatography  
142 (FPLC) performed with an ÄKTA-Purifier system according to the method of Si Ahmed Zennia et  
143 al. (2015). The native form (A<sub>1</sub>) was also purified by anion-exchange FPLC, but from the soluble  
144 proteins that had not been incubated at 37 °C. The recovered  $\alpha$ -La isoforms were then checked for  
145 purity by native polyacrylamide gel electrophoresis (PAGE performed under non-reducing and non-  
146 denaturing conditions) as described (Si Ahmed Zennia et al., 2015). The three isoforms were desalted  
147 by size exclusion chromatography onto a Superdex 75 column connected to the ÄKTA-FPLC system  
148 stored in a refrigerated cabinet maintained at 4 °C, and finally concentrated with an Amicon™  
149 concentration cell.

150

## 151 2.3. Circular dichroism of $\alpha$ -La isoforms

152

153 The circular dichroism (CD) spectra were recorded with a spectropolarimeter CD6 equipped  
154 with a thermostatic cell holder (25 °C), using 1.0-mm path length quartz cell. CD spectra were

155 acquired with 20-nm/min scan speed at 0.2 nm step size and 1.0-nm bandwidth under constant  
156 purging with nitrogen. Changes in the secondary structures of deamidated forms of camel  $\alpha$ -La were  
157 monitored in the far-UV region (190–260 nm) at final protein solutions concentration of 36, 63 and  
158 76  $\mu$ M for A<sub>1</sub>, A<sub>2</sub>, and A<sub>3</sub> isoforms, respectively. Near-UV CD (260–320 nm) spectra were recorded  
159 using the same parameters with final protein concentrations of 3.60, 12.70 and 7.65  $\mu$ M for A<sub>1</sub>, A<sub>2</sub>,  
160 and A<sub>3</sub> isoforms, respectively. The concentration of protein solutions was measured  
161 spectrophotometrically using an extinction coefficient of  $\epsilon = 32,470 \text{ M}^{-1} \text{ cm}^{-1}$  at 280 nm. The buffer  
162 was sodium phosphate 10 mM, pH 7.4. Three spectra were accumulated and averaged for each  
163 sample. The baseline obtained with buffer was subtracted from each spectrum and the resultant  
164 values were adjusted to the concentration when mdeg expressed raw data were converted to mean  
165 residue ellipticity  $[\theta]$  expressed in  $\text{deg cm}^2 \text{ dmol}^{-1}$ , based on a mean amino acid residue molecular  
166 mass ( $m$ ) of 113 Da. The mean residue ellipticity was defined as:

167

$$168 \quad [\theta]_{\lambda} = 100 m \theta_{\text{obs}} c/l \quad (1)$$

169

170 where  $\theta_{\text{obs}}$  is the observed ellipticity in degrees at a given wavelength,  $c$  is the protein concentration  
171 in mg/mL and  $l$  is the length of the cell (cm). Secondary structure estimation from the far-UV CD  
172 spectra was calculated using the software CDNN (Böhm, Muhr, & Jaenicke, 1992).

173

## 174 *2.4. Crystal structure of camel $\alpha$ -La*

### 175 *2.4.1. Crystallization and X-ray data collection*

176

177 Crystals of camel  $\alpha$ -La were grown by vapor diffusion in hanging drops according to Ducruix  
178 and Giegé (1999). Drops were made at 293 K by mixing 2  $\mu$ L of the protein solution at 45 mg/mL  
179 and 3  $\mu$ L of a reservoir solution containing 20% polyethylene glycol PEG 6000, 2 mM zinc chloride,



180 and 100 mM Tris at pH 8.0. The obtained crystals belong to space group  $P3_121$  with unit-cell  
181 parameters  $a = 52.2 \text{ \AA}$ ,  $b = 52.2 \text{ \AA}$ , and  $c = 75.5 \text{ \AA}$ . Assuming one monomer in the asymmetric unit,  
182 the packing density  $V_M$  is  $2.06 \text{ \AA}^3 \cdot \text{Da}^{-1}$  and the solvent content is 40.3%. Crystals were flash frozen  
183 in liquid nitrogen in the mother liquor with addition of 20% glycerol as cryoprotectant. A native data  
184 set at  $1.93\text{-\AA}$  resolution was collected in our laboratory at 100 K on an X8-Proteum diffractometer,  
185 with incident radiation at a wavelength of  $1.542 \text{ \AA}$ . The crystal-to-detector distance was 40 mm with  
186  $0.5^\circ$  oscillation per CCD image. Data were processed using the X8-Proteum<sup>Plus</sup> software from Bruker  
187 AXS.

188

#### 189 2.4.2. Crystal structure determination

190

191 The crystal structure of the camel  $\alpha$ -La was solved by molecular replacement with the  
192 program PHASER (McCoy et al., 2007) using the coordinates of the human  $\alpha$ -La (Chandra et al.,  
193 1998; PDB 1A4V). Building of the model was performed using Coot (Emsley, Lohkamp, Scott, &  
194 Cowtan, 2010), and the refinement of the crystal structure was performed in the range  $10\text{--}1.93 \text{ \AA}$   
195 using REFMAC5 (Vagin et al., 2004). A total of 10% of the native data were selected for  $R_{\text{free}}$   
196 calculations. The model was refined to the final  $R_{\text{factor}}$  of 19.5% and  $R_{\text{free}}$  of 26.8% (Table S1) and  
197 includes residues 1–43, 46–65, and 68–120 of the camel  $\alpha$ -La, as well as 84 water molecules, one  
198 calcium ion, and one zinc ion. Because of the lack of density, residues 44–45, 66–67, and 121–123 of  
199 the camel  $\alpha$ -La were not built. Over 96% of the residues were within the most favored regions, and  
200 no residue was within the disallowed regions in a Ramachandran plot, as defined by PROCHECK  
201 (Laskowski, McArthur, Moss, & Thornton, 1993).

202

#### 203 2.5. Differential scanning calorimetry of $\alpha$ -La isoforms

204

205 Differential Scanning Calorimetry (DSC) experiments were performed on a Microcal VP-  
206 DSC apparatus equipped with 0.54-mL cells, at pressure of 2 atm. The thermograms were recorded  
207 using the isoforms A<sub>1</sub>, A<sub>2</sub> and A<sub>3</sub> of  $\alpha$ -La at a 0.5 mg/mL (35  $\mu$ M) in 10 mM acetate buffer pH 6.0.  
208 A scanning window from 20 to 100 °C with a constant scan rate of 1 °C/min was applied. Origin 7.0  
209 software was used to determine the T<sub>m</sub> (midpoint of the unfolding transition) and the  $\Delta H_{cal}$   
210 (calorimetric enthalpy). Except for the A1 isoform, reversibility of unfolding was observed when the  
211 samples were rescanned after heating to 100 °C. Baselines recorded with both cells filled with buffer  
212 were subtracted from the experimental traces to obtain the heat capacity curves ( $\Delta C_p$ , excess heat  
213 capacity, vs. temperature). The thermodynamic data were the average of three scans and results were  
214 expressed as the mean  $\pm$  SD. Statistical analysis was performed with GraphPad Prism 5 using one-  
215 way ANOVA method followed by Bonferroni's multiple comparison test.

216

## 217 2.6. Susceptibility of $\alpha$ -La isoforms to thermolysin hydrolysis

218

219 Hydrolysis of the camel  $\alpha$ -La isoforms A<sub>1</sub>, A<sub>2</sub>, and A<sub>3</sub> by thermolysin (EC 3.4.24.27) was  
220 carried out according to N'Negue et al. (2006). The  $\alpha$ -La isoforms (A<sub>1</sub>, A<sub>2</sub>, and A<sub>3</sub>) were solubilized  
221 at 1 mg/mL (70  $\mu$ M) in 50 mM 2-[4-(2-hydroxyethyl)-1-piperazine] ethanesulfonate buffer, pH 7.2,  
222 containing 10 mM CaCl<sub>2</sub> and 0.02% sodium azide. An appropriate aliquot of thermolysin from  
223 *Bacillus thermoproteolyticus rokko* was added to 1 mL of each  $\alpha$ -La isoform solution to obtain an  
224 enzyme-to-substrate molar ratio of 1/80. The reaction was carried out at 37 °C for 30 to 180 min and  
225 was stopped by adding 2% trifluoroacetic acid which decreased the pH to 1.0. The characterization  
226 of the hydrolyzates obtained from each  $\alpha$ -La isoform was performed by reversed-phase high-  
227 performance liquid chromatography (HPLC) onto a LichroCart C<sub>18</sub> column connected to an Alliance  
228 2690 unit according to N'Negue et al. (2006). Bovine  $\alpha$ -La, purified from raw milk as previously  
229 described (N'Negue et al., 2006), was used as the reference in the same experimental conditions.

230

### 231 **3. Results and discussion**

232

233 In a previous work (Si Ahmed Zennia et al., 2015), we unveiled that camel  $\alpha$ -La (Swiss-Prot  
234 accession number P00710) is subject to nonenzymatic deamidation at its two Asn-Gly motifs, Asn<sup>45</sup>  
235 being more readily deamidated than Asn<sup>16</sup> for which a more basic pH is needed for the generation of  
236 the deamidated form. Besides, we demonstrated that the two variants reported in the earlier literature  
237 correspond in fact to native isoform (A<sub>1</sub>) and to mono-deamidated isoform at position 45 (A<sub>2</sub>). No di-  
238 deamidated isoform (A<sub>3</sub>) was observed in the early reports. The present paper focuses on the impact  
239 of deamidation on the structure of camel  $\alpha$ -La, this nonenzymatic modification being the most  
240 extensive among all  $\alpha$ -Las susceptible to deamidation.

241 The three isoforms were prepared by anion-exchange FPLC with high purity as shown by  
242 native PAGE analysis (Fig. 1). Their identification was performed by determination of their  
243 respective molecular masses in our previous work (Si Ahmed Zennia et al., 2015). Differences in  
244 molecular masses between A<sub>1</sub> and A<sub>2</sub>, and between A<sub>2</sub> and A<sub>3</sub> are 0.991 and 0.984 Da, respectively,  
245 that corresponds to the replacement of one primary amine function by one hydroxyl function in the  
246 case of deamidation of one Asn residue. Besides, the calcium ion naturally bound to the protein was  
247 preserved during the chromatographic purification step performed under nondenaturing conditions.  
248 Indeed, Girardet et al. (2004) showed that the addition of ethylenediaminetetraacetate (EDTA, strong  
249 chelator of calcium) to equine  $\alpha$ -La leads to release of calcium ion, observed electrophoretically by a  
250 band shift of the  $\alpha$ -La, deamidated or not (higher migration rate). Thus, the native and deamidated  $\alpha$ -  
251 La isoforms are still in their holo form after their purification. Two other studies (Salami et al., 2009;  
252 Atri et al., 2010) have also purified the holo form of camel  $\alpha$ -La without loss of calcium ion during  
253 the process (ammonium sulfate precipitation and ultrafiltration). In fact, the calcium ion strongly  
254 binds to  $\alpha$ -La with an affinity constant of  $3 \times 10^8 \text{ M}^{-1}$  for human  $\alpha$ -La (Permyakov & Berliner,  
255 2000).

256 The secondary and tridimensional structures of A<sub>1</sub>, A<sub>2</sub>, and A<sub>3</sub> were investigated by CD in the  
257 far- and near-UV regions (Fig. 2). The near-UV CD spectra had the typical features of the spectrum  
258 of holo- $\alpha$ -La with a minimum in the region 270–275 nm (corresponding to Tyr) and a maximum at  
259 292 nm for Trp (Girardet et al., 2004; N'Negue et al., 2006; Saricay, Wierenga, & de Vries, 2014).  
260 According to former studies, the spectrum of apo- $\alpha$ -La is different but nevertheless retains the  
261 characteristic shape of the spectrum of the holo- $\alpha$ -La with much lower intensity (Saricay et al.,  
262 2014), or is featureless (N'Negue et al., 2006). However, the peak at 292 nm was not well-resolved  
263 in the case of the camel  $\alpha$ -La, because the signal related to 5 Trp (the camel protein contains an extra  
264 Trp) is stronger around 300 nm than the signal due to only 4 Trp in the case of bovine  $\alpha$ -La  
265 (N'Negue et al., 2006; Saricay et al., 2014) or equine  $\alpha$ -La (Girardet et al., 2004). On the other hand,  
266 the spectra of the three isoforms were similar suggesting that the single deamidation as well as the  
267 double deamidation had no significant effect on the 3D structure of camel  $\alpha$ -La, or as no aromatic  
268 amino acid is sufficiently close to the deamidation sites, no disturbance of the aromatic amino acid  
269 environment was detected.

270 The far-UV spectra of A<sub>1</sub>, A<sub>2</sub>, and A<sub>3</sub> corresponded to ordered secondary structures with  
271 more than 52% of  $\alpha$ -helices and  $\beta$ -strands (Table 1). The shapes of the spectra were similar to those  
272 determined by Salami et al. (2009) and Atri et al. (2010) for camel holo- $\alpha$ -La in native state. When  
273 the protein became deamidated, the ellipticity at 222 nm increased, that could be interpreted by an  
274 increase of  $\alpha$ -helix content upon deamidation (Greenfield, 2006). The deamidation of Asn<sup>45</sup> (isoform  
275 A<sub>2</sub>) seemed to be the one that caused the most pronounced conformational change with this particular  
276 gain in  $\alpha$ -helix secondary structure. The extra deamidation of Asn<sup>16</sup> (in A<sub>3</sub>) did not seem to modify  
277 more significantly the conformation at the secondary structure level. It is worthy to note that the  
278 secondary structure content of A<sub>2</sub> is very close to that of the camel  $\alpha$ -La in Atri et al. (2010),  
279 suggesting that the reported protein is perhaps mono-deamidated. Besides, the secondary structure  
280 content of A<sub>2</sub> was also close to that of its bovine counterpart (Atri et al., 2010).

281 In order to deepen the structural investigations, we determined the 3D structure of the camel  
282  $\alpha$ -La at atomic resolution by X-ray crystallography. The overall fold of the camel  $\alpha$ -La (Fig. 3a) is  
283 similar to the 3D structure of other  $\alpha$ -La from various species. For instance, the superimposition of  
284 the 3D structure of the camel  $\alpha$ -La with the crystal structures of the human  $\alpha$ -La (Chrysina et al.,  
285 2000) and the bovine  $\alpha$ -La (Chandra et al., 1998) yielded a root-mean-square deviation of C $\alpha$   
286 positions of 0.79 Å and 0.83 Å, respectively. The crystal structure of the camel  $\alpha$ -La revealed the  
287 presence of one calcium ion at the surface of the protein. This calcium binding-site was identical to  
288 that found in the crystal structures of human and bovine  $\alpha$ -Las and involved side-chains of Asp<sup>82</sup>,  
289 Asp<sup>87</sup> and Asp<sup>88</sup>. As the solution used for the crystallization of the camel  $\alpha$ -La did not contain  
290 calcium ions (see Materials and Methods), the calcium ion was not lost during the chromatography  
291 purification step and the camel  $\alpha$ -La was still in its holo form after purification. The crystals of  
292 camel  $\alpha$ -La that were used for X-ray structure determination, were obtained from pure  $\alpha$ -La isoform  
293 A<sub>1</sub> (no deamidation) in a solution containing 100 mM Tris at pH 8.0. As the Asn<sup>45</sup> from camel  $\alpha$ -La  
294 was shown to deamidate spontaneously at pH 7.4 whereas Asn<sup>16</sup> needs a more basic pH upper to 8.0  
295 to undergo a deamidation process (Si Ahmed Zennia et al., 2015), a native PAGE analysis of the  
296 crystals was performed to determine which  $\alpha$ -La isoform was preferentially crystallized. As shown  
297 in Figure 3b, mainly the mono-deamidated isoform A<sub>2</sub> (deamidation of Asn<sup>45</sup>) was generated during  
298 the crystallogenesis. The deamidation of Asn led to the production of a mixture of L-isoAsp, L-Asp,  
299 D-isoAsp, and D-Asp residues in the polypeptide chain (Aswad et al., 2000). A lack of electron  
300 density was observed in the crystal structure of camel  $\alpha$ -La for the loop between  $\beta$ -strands  $\beta$ 2 and  $\beta$ 3  
301 that includes Asn<sup>45</sup> and this could be explained by an heterogeneity in the sample due to spontaneous  
302 deamidation in the crystal (Fig. 3b), whereas a clear electron density was observed for the loop  
303 between  $\alpha$ -helices  $\alpha$ 1 and  $\alpha$ 2 where Asn<sup>16</sup> is located. Thus, the crystal structure of the camel  $\alpha$ -La  
304 determined in the present study corresponded to the isoform A<sub>2</sub> with the deamidation of Asn<sup>45</sup> and no  
305 deamidation of Asn<sup>16</sup>.

306 In accordance with results of near-UV CD spectra of isoforms A<sub>1</sub> and A<sub>2</sub>, the single  
307 deamidation had no significant effect on the overall fold of the camel  $\alpha$ -La. However, a close  
308 structural comparison of the camel  $\alpha$ -La with bovine and human  $\alpha$ -Las revealed the existence of a  
309 small additional  $\alpha$ -helix (named  $\alpha$ 4) in the camel  $\alpha$ -La that included residues 101 to 106. These  
310 residues are located in, or close to the flexible loop 105–110 (Chandra et al., 1998; Chrysina et al.,  
311 2000) and this could explain that these residues 101–106 were prone to adopt a helical conformation  
312 under particular conditions such as deamidation. As described above, the far-UV CD spectra of the  
313 isoforms A<sub>1</sub> and A<sub>2</sub> of the camel  $\alpha$ -La showed that this protein underwent slightly increase of the  $\alpha$ -  
314 helix content upon deamidation as confirmed by the increasing 222 nm value. Interestingly, the  
315 additional  $\alpha$ -helix  $\alpha$ 4 was located at the proximity of the Asn<sup>45</sup> deamidation site in the crystal  
316 structure of the camel  $\alpha$ -La (Fig. 3a) and such a deamidation process might modify the local  
317 physicochemical properties of the protein in the vicinity of the loop  $\beta$ 2- $\beta$ 3 that includes the  
318 deamidation site. Overall, these results suggested that the deamidation of Asn<sup>45</sup> (isoform A<sub>2</sub>) seemed  
319 to induce the formation of this additional short  $\alpha$ -helix in camel  $\alpha$ -La.

320 A DSC approach was used to study the thermostability of the camel  $\alpha$ -La upon deamidation  
321 (Fig. 4). The DSC thermograms underwent significant shifts as a function of deamidation level (from  
322 0 to 2). As the protein was deamidated, it became more heat stable: the melting temperature (T<sub>m</sub>)  
323 increased significantly ( $p < 0.01$ ) by ca. 3 °C per deamidation level (Table 1). The enthalpy change  
324 ( $\Delta H_{cal}$ ) did not differ significantly from an isoform to another, suggesting that same amount of  
325 energy was necessary for their unfolding. However, the consequences on the physical features were  
326 drastically different, since the native  $\alpha$ -La (A<sub>1</sub>) precipitated at temperatures higher than 80 °C  
327 contrary to the deamidated isoforms (A<sub>2</sub> and A<sub>3</sub>) for which the denaturation process was reversible  
328 between 20 and 100 °C. Extra negative charges carried by the isoAsp or Asp residues would  
329 strengthen the intramolecular electrostatic interactions of the  $\alpha$ -La molecule. The conclusions of  
330 Atri, Saboury, Moosavi-Movahedi, Kavousi, and Ariaeenejad (2015) substantiate this possible

331 explanation. Indeed, the authors observed that binding of zinc ion onto a secondary site of camel  $\alpha$ -  
332 La decreases thermal stability, as intramolecular electrostatic interactions weaken. This secondary  
333 binding site is identified in human  $\alpha$ -La and concerns in particular residues Glu<sup>49</sup> and Glu<sup>116</sup> located  
334 on the surface of the molecule (Noyelle & Van Dael, 2002). In our opinion, the addition of negative  
335 charges (by deamidation) should have an opposite effect to Zn binding that shields a number of  
336 negative charges on the thermostability of camel  $\alpha$ -La. Besides, it is noteworthy that the melting  
337 temperature ( $T_m$ ) and enthalpy change ( $\Delta H_{cal}$ ) determined for the mono-deamidated protein A<sub>2</sub> were  
338 very close to those of the camel  $\alpha$ -La reported by Atri et al. (2010), supporting the hypothesis that  
339 the  $\alpha$ -La of their study might have deamidated spontaneously.

340 On the other hand, the thermodynamic parameters of native camel  $\alpha$ -La A<sub>1</sub> were rather close  
341 to those determined for the bovine  $\alpha$ -La (Atri et al., 2010). Nevertheless and unlike the native  
342 isoform A<sub>1</sub>, the thermal denaturation of the bovine protein is reversible between 15 and 100 °C,  
343 according to Boye, Alli, and Ismail (1997). The ability of bovine holo- $\alpha$ -La to renature upon cooling  
344 is attributed to the absence of aggregation upon thermal treatment. The secondary structure of the  
345 bovine  $\alpha$ -La is easily altered by heating but can refold to a conformation similar to that of its native  
346 state (Boye et al., 1997). This could explain why Felfoul, Lopez, Gaucheron, Attia, and Ayadi (2015)  
347 have observed that camel  $\alpha$ -La precipitates more easily than bovine  $\alpha$ -La upon milk heat treatment  
348 mimicking industrial conditions. With a less ordered secondary structure, the native  $\alpha$ -La (isoform  
349 A<sub>1</sub>) was readily prone to precipitate at high temperature, but not the bovine counterpart. It would  
350 seem that the deamidation process would prevent aggregation and precipitation of the camel protein  
351 at high temperature by inducing a conformational change resulting in a more ordered secondary  
352 structure (additional  $\alpha$ -helix  $\alpha_4$  in isoform A<sub>2</sub>).

353 Due to its compact structure, bovine  $\alpha$ -La is known to be resistant to proteolytic enzymes,  
354 and especially to thermolysin, a thermostable enzyme (N'Negue et al., 2006). Thus, the impact of  
355 deamidation on the susceptibility of camel  $\alpha$ -La towards thermolytic activity was studied in the

356 present work. It is reported that the bovine  $\alpha$ -La, in its folded state, is highly resistant to thermolysin  
357 at temperatures reaching up to at least 44 °C (N'Negue et al., 2006). The enzyme possesses  
358 endopeptidase activity and cleaves the peptide bonds of bovine  $\alpha$ -La (unfolded) preferentially at the  
359 amino-terminal side of the hydrophobic residues Ile, Leu, Phe, Tyr and, to a lesser extent of Val  
360 (N'Negue et al., 2006). The bovine  $\alpha$ -La is sensitive to thermolysin only in a molten globule state,  
361 for which the hydrophobic clusters are more accessible. Indeed, at a temperature of 70 °C, the bovine  
362 protein adopts a partly unfolded, reversible state and its hydrolysis is readily achieved by thermolysin  
363 (N'Negue et al., 2006). The present work shows that camel  $\alpha$ -La was also resistant to thermolysin,  
364 similarly to the bovine protein, as few peptides were released after incubation for 3 h at 37 °C (Fig.  
365 5). The camel protein was folded in a compact structure conferring this resistance. The nonenzymatic  
366 deamidation did not change the behaviour of camel  $\alpha$ -La toward the thermolysin, as similar HPLC  
367 profiles were obtained between the three isoforms A<sub>1</sub>, A<sub>2</sub>, and A<sub>3</sub> (Fig. 5). The fact that the  
368 deamidated isoforms were equally resistant to thermolysin was expected, because the altered proteins  
369 adopted a slightly more ordered secondary structure while keeping the native 3D structure, and also  
370 acquired conformations more stable toward heat treatment. The altered isoforms might not expose  
371 their hydrophobic clusters to the solvent, so that aggregation and subsequent precipitation upon  
372 thermal treatment did not occur, on the contrary to the native isoform, and the sites of hydrolysis by  
373 thermolysin were kept hidden in the structure. Salami et al. (2009) reported that the pancreatic  
374 enzymes, i.e., trypsin and chymotrypsin, are able to partly degrade camel  $\alpha$ -La *in vitro*, the latter  
375 being a better substrate than the bovine counterpart, both in the native and molten globule states.  
376 Trypsin was also used in the present study (data not shown). As observed with thermolysin, the  
377 camel  $\alpha$ -La isoforms displayed a relative resistance to trypsin with similar HPLC profiles (i.e. few  
378 peptides generated and significant remaining protein).

379 After camel milk or milk-derived food intake, the  $\alpha$ -La might undergo a deamidation  
380 mechanism in the gut, the physiological conditions, i.e., pH 7.0–8.0, and 37 °C, being favorable for  
381 this process to take place. The altered protein would be resistant to pancreatic proteases or brush-



382 border membrane peptidases in the intestinal tract, and might acquire biological activity, for instance  
383 against cancer cells, in a way similar to HAMLET (Ho et al., 2017) or camel oleic acid-binding  $\alpha$ -La  
384 (Atri et al., 2011; Uversky et al., 2017). If case the  $\alpha$ -La is hydrolyzed, the generated peptides with  
385 an Asn-Gly motif are more readily prone to deamidate, as they lack ordered secondary structure that  
386 inhibits the nonenzymatic deamidation in proteins (Robinson & Robinson, 2004). Thus, peptides  
387 containing the Asn<sup>16</sup>-Gly<sup>17</sup> sequence would be more easily deamidated in the gut, whereas the  
388 reaction is limited in the whole protein. This would result in accumulation of unusual residues such  
389 as L/D-isoAsp and D-Asp that might either have a deleterious effect in term of food allergy or gain  
390 some benefits, for instance in the recognition of integrins overexpressed in the membrane of tumor  
391 cells. In this context, it is interesting to note that the motifs isoAsp-Gly-Asn-Arg or Asp-Gly-Asn-  
392 Arg at position 45–48 of the camel  $\alpha$ -La presents similarities to sequences isoAsp-Gly-Arg  
393 (Mastrangeli et al., 2018) and Arg-Gly-Asp (Polo et al., 2018) that bind efficiently to some members  
394 of the integrin family, as very recently reported.

395

#### 396 **4. Conclusion**

397

398 The  $\alpha$ -La of the *Camelidae* family is the only one that possesses two sites of nonenzymatic  
399 deamidation among the known  $\alpha$ -Las in other mammals. Devoid of Asn-Gly sequence, the bovine  $\alpha$ -  
400 La does not deamidate spontaneously and remains chemically stable. The present study focused on  
401 the impact of the deamidation on the structure and stability of camel  $\alpha$ -La. This post-translational  
402 modification reinforced the stability of the protein toward heat treatment and preserved the resistance  
403 toward proteolysis. Our experimental findings suggest that the deamidation process is able to induce  
404 a conformational change with an extra  $\alpha$ -helix in the C-terminal region that conferred higher stability  
405 of the protein. To understand the biological significance of this kind of chemical alteration, further  
406 investigations on the bioavailability and health impact of the camel  $\alpha$ -La need to be performed.

407

408 **Acknowledgements**

409

410 The stay of Dr. S. Si Ahmed Zennia in University of Lorraine (Vandœuvre-lès-Nancy,  
411 France) was supported by the Mouloud Mammeri University of Tizi-Ouzou (Algeria). The authors  
412 thank Ouargla Kasdi Merbah University (Algeria) for the gift of camel milk. The biophysics and  
413 structural biology results were obtained with the help of the UMS2008 IBSLor platform. The authors  
414 thank Prof. Jean-Pierre Jacquot (University of Lorraine) for the revision of the manuscript and Prof.  
415 Pascal Reboul and Dr. Arnaud Bianchi (University of Lorraine) for their help in the statistical  
416 analyses.

417

418 **References**

419

420 Alavi, F., Salami, M., Emam-Djomeh, Z., & Mohammadian, M. (2017). Nutraceutical properties of  
421 camel milk. In R. Watson, R. J. Collier, & V. Preedy (Eds.), *Nutrients in dairy and their implications*  
422 *on health and disease* (pp. 451–458). San Diego: Academic Press.

423 Aswad, D. W., Paranandi, M. V., & Schurter, B. T. (2000). Isoaspartate in peptides and proteins:  
424 Formation, significance, and analysis. *Journal of Pharmaceutical and Biomedical Analysis*, *21*,  
425 1129–1136.

426 Atri, M. S., Saboury, A. A., Moosavi-Movahedi, A. A., Goliaei, B., Sefidbakht, Y., Alijanvand, H. H.,  
427 et al. (2011). Structure and stability analysis of cytotoxic complex of camel  $\alpha$ -lactalbumin and  
428 unsaturated fatty acids produced at high temperature. *Journal of Biomolecular Structure and*  
429 *Dynamics*, *28*, 919–928.

430 Atri, M. S., Saboury, A. A., Moosavi-Movahedi, A. A., Kavousi, K., & Ariaeenejad, S. (2015).  
431 Effects of zinc binding on the structure and thermal stability of camel  $\alpha$ -lactalbumin. *Journal of*  
432 *Thermal Analysis and Calorimetry*, *120*, 481–488.

433 Atri, M. S., Saboury, A. A., Yousefi, R., Dalgalarondo, M., Chobert, J.-M., Haertlé, T., et al. (2010).  
434 Comparative study on heat stability of camel and bovine apo and holo  $\alpha$ -lactalbumin. *Journal of*  
435 *Dairy Research*, 77, 43–49.

436 Belizy, S., Nasarova, I. N., Procof'ev, V. N., Sorokina, I. A., Puschkina, N. V., & Lukach, A. I.  
437 (2001). Changes in antioxidative properties of lactoferrin from women's milk during deamidation.  
438 *Biochemistry (Moscow)*, 66, 576–580.

439 Böhm, G., Muhr, R., & Jaenicke, R. (1992). Quantitative analysis of protein far UV circular  
440 dichroism spectra by neural networks. *Protein Engineering, Design and Selection*, 5, 191–195.

441 Boye, J. I., Alli, I., & Ismail, A. A. (1997). Use of differential scanning calorimetry and infrared  
442 spectroscopy in the study of thermal and structural stability of  $\alpha$ -Lactalbumin. *Journal of*  
443 *Agricultural and Food Chemistry*, 45, 1116–1125.

444 Chandra, N., Brew, K., & Acharya, K .R. (1998). Structural evidence for the presence of a secondary  
445 calcium binding site in human  $\alpha$ -lactalbumin. *Biochemistry*, 37, 4767–4772.

446 Chrysina, E. D., Brew, K., & Acharya, K. R. (2000). Crystal structures of apo- and holo-bovine  $\alpha$ -  
447 lactalbumin at 2.2 Å resolution reveal an effect of calcium on inter-lobe interactions. *Journal of*  
448 *Biology and Chemistry*, 275, 37021–37029.

449 Ducruix, A. & Giegé, R. (1999). Methods of crystallization. In A. Ducruix & R. Giegé (Eds.),  
450 *Crystallization of nucleic acids and proteins: A practical approach*, 2<sup>nd</sup> ed. (pp. 121-147). Oxford:  
451 IRL Press.

452 Emsley, P., Lohkamp, B., Scott, W. G., & Cowtan, K. (2010). Features and development of Coot.  
453 *Acta Crystallographica. Section D, Biological Crystallography*, 66, 486–501.

454 Felfoul, I., Lopez, C., Gaucheron, F., Attia, H., & Ayadi, M. A. (2015). Fouling behavior of camel  
455 and cow milks under different heat treatments. *Food and Bioprocess Technology*, 8, 1771–1778.

456 Gall, H., Kalveram, C. M., Sick, H., & Sterry, W. (1996). Allergy to the heat-labile proteins  $\alpha$ -  
457 lactalbumin and  $\beta$ -lactoglobulin in mare's milk. *Journal of Allergy and Clinical Immunology*, 97,  
458 1304–1307.

459 Girardet, J.-M., Miclo, L., Florent, S., Mollé, D., & Gaillard, J.-L. (2006). Determination of the  
460 phosphorylation level and deamidation susceptibility of equine  $\beta$ -casein. *Proteomics*, *6*, 3707–3717.

461 Girardet, J.-M., N'Negue, M.-A., Egito, A. S., Campagna, S., Lagrange, A., & Gaillard, J.-L. (2004).  
462 Multiple forms for equine  $\alpha$ -lactalbumin: Evidence of N-glycosylated and deamidated forms.  
463 *International Dairy Journal*, *14*, 207–217.

464 Greenfield, N. J. (2006). Using circular dichroism spectra to estimate protein secondary structure.  
465 *Nature Protocols*, *1*, 1754–2189.

466 Ho, J. C. S., Nadeem, A., & Svanborg, C. (2017). HAMLET - A protein-lipid complex with broad  
467 tumoricidal activity. *Biochemical and Biophysical Research Communications*, *482*, 454–458.

468 Kuhn, N. J., Carrick, D. T., & Wilde, C. J. (1980). Lactose synthesis – Possibilities of regulation.  
469 *Journal of Dairy Science*, *63*, 328–336.

470 Laskowski, R. A., McArthur, M. W., Moss, D. S., & Thornton, J. M. (1993). PROCHECK: a  
471 program to check the stereochemical quality of protein structures. *Journal of Applied*  
472 *Crystallography*, *26*, 283–291.

473 Lindberg, T., Engberg, S., Sjöberg, L. B., & Lönnerdal, B. (1998). In vitro digestion of proteins in  
474 human milk fortifiers and in preterm formula. *Journal of Pediatric Gastroenterology and Nutrition*,  
475 *27*, 30–36.

476 Mastrangeli, M., D'amici, F., D'Acunto, C.-W., Fiumi, S., Rossi, M., Terlizze, M., et al. (2018). A  
477 deamidated interferon- $\beta$  variant binds to integrin  $\alpha v\beta 3$ . *Cytokine*, *104*, 38–41.

478 McCoy, A. J., Grosse-Kunstleve, R. W., Adams, P. D., Winn, M. D., Storoni, L. C., & Read, R. J.  
479 (2007). Phaser crystallographic software. *Journal of Applied Crystallography*, *40*, 658–674.

480 Meltretter, J., Wüst, J., & Pisc, M. (2013). Comprehensive analysis of nonenzymatic post-  
481 translational  $\beta$ -lactoglobulin modifications in processed milk by ultra high performance liquid  
482 chromatography-tandem mass spectrometry. *Journal of Agricultural and Food Chemistry*, *61*,  
483 6971–6981.

484 Natale, M., Bisson, C., Monti, G., Peltran, A., Perono Garoffo, L., Valentini, S., et al. (2004). Cow's  
485 milk allergens identification by two-dimensional immunoblotting and mass spectrometry. *Molecular*  
486 *Nutrition and Food Research*, 48, 363–369.

487 N'Negue, M.-A., Miclo, L., Girardet, J.-M., Campagna, S., Molle, D., & Gaillard J.-L. (2006).  
488 Proteolysis of bovine  $\alpha$ -lactalbumin by thermolysin during thermal denaturation. *International Dairy*  
489 *Journal*, 16, 1157–1167.

490 Nonaka, Y., Aizawa, T., Akieda, D., Yasui, M., Watanabe, M., Watanabe, N., et al. (2008).  
491 Spontaneous asparaginyl deamidation of canine milk lysozyme under mild conditions. *Proteins*, 72,  
492 313–322.

493 Noyelle, K., & Van Dael, H. (2002). Kinetics of conformational changes induced by the binding of  
494 various metal ions to bovine  $\alpha$ -lactalbumin. *Journal of Inorganic Biochemistry*, 88, 69–76.

495 Permyakov, E. A., & Berliner, L. J. (2000).  $\alpha$ -Lactalbumin: Structure and function. *FEBS Letters*,  
496 473, 269–274.

497 Polo, E., Nitka, T. T., Neubert, E., Erpenbeck, L., Vuković, L., & Kruss, S. (2018). Control of  
498 Integrin Affinity by Confining RGD Peptides on Fluorescent Carbon Nanotubes. *ACS Applied*  
499 *Materials and Interfaces*, 10, 17693–17703.

500 Ptitsyn, O. B. (1995). Molten globule and protein folding. *Advances in Protein Chemistry*, 47,  
501 83–229.

502 Robinson, N. E., & Robnson, A. B. (2004). *Molecular Clocks: Deamidation of Asparaginyl and*  
503 *Glutaminyl Residues in Peptides and Proteins*. Cave Junction: Althouse Press.

504 Sakandar, H. A., Ahmad, S., Perveen, R., Aslam, H. K. W., Shakeel, A., Sadiq, F. A., et al. (2018).  
505 Camel milk and its allied health claims: a review. *Progress in Nutrition*, 20, 15–29.

506 Salami, M., Yousefi, R., Ehsani, M. R., Razavi, S. H., Chobert, J.-M., Haertlé, T., et al. (2009).  
507 Enzymatic digestion and antioxidant activity of the native and molten globule states of camel  $\alpha$ -  
508 lactalbumin: Possible significance for use in infant formula. *International Dairy Journal*, 19,  
509 518–523.

510 Saricay, Y., Wierenga, P. A., & de Vries, R. (2014). Changes in protein conformation and surface  
511 hydrophobicity upon peroxidase-catalyzed cross-linking of apo- $\alpha$ -lactalbumin. *Journal of*  
512 *Agricultural and Food Chemistry*, 62, 9345–9352.

513 Schmidt, D. G. & Poll, J. K. (1991). Enzymatic hydrolysis of whey proteins. Hydrolysis of  $\alpha$ -  
514 lactalbumin and  $\beta$ -lactoglobulin in buffer solutions by proteolytic enzymes. *Netherlands Milk and*  
515 *Dairy Journal*, 45, 225–240.

516 Si Ahmed Zennia, S., Mati, A., Saulnier, F., Verdier Y., Chiappetta, G., Mulliert, G., et al. (2015).  
517 Identification by FT-ICR-MS of *Camelus dromedarius*  $\alpha$ -lactalbumin variants as the result of  
518 nonenzymatic deamidation of Asn-16 and Asn-45. *Food Chemistry*, 187, 305–313.

519 Uversky, V. N., El-Fakharany, E. M., Abu-Serie, M. M., Almehdar, H. A., & Redwan, E. M. (2017).  
520 Divergent anticancer activity of free and formulated camel milk  $\alpha$ -lactalbumin. *Cancer Investigation*,  
521 35, 610–623.

522 Vagin, A. A., Steiner, R. A., Lebedev, A. A., Potterton, L., McNicholas, S., Long, F. et al. (2004).  
523 REFMAC5 dictionary: organization of prior chemical knowledge and guidelines for its use. *Acta*  
524 *Crystallographica. Section D, Biological Crystallography*, 60, 2184–2195.

525 Wu, X., Lu, Y., Xu, H., Lin, D., He, Z., Wu, H., et al. (2018). Reducing the allergenic capacity of  $\beta$ -  
526 lactoglobulin by covalent conjugation with dietary polyphenols. *Food Chemistry*, 256, 427–434.

527

528

## Legends to Figures

529

530 **Fig.1.** Native PAGE control of native ( $A_1$ ), mono-deamidated ( $A_2$ ), and di-deamidated ( $A_3$ )  $\alpha$ -La  
531 purified by anion-exchange FPLC. IgG, immunoglobulins G; SA, serum albumin; SP, total soluble  
532 proteins of camel milk.

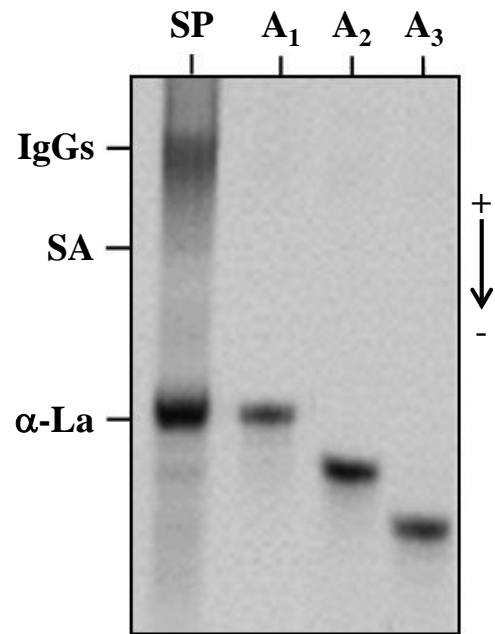
533 **Fig. 2.** CD spectra of native ( $A_1$ ), mono-deamidated ( $A_2$ ), and di-deamidated ( $A_3$ )  $\alpha$ -La in the far-UV  
534 (a) and near-UV (b) regions.  $[\theta]$ , mean residue ellipticity.

535 **Fig. 3.** (a) Ribbon representation of the camel  $\alpha$ -La crystal structure with  $\alpha$ -helices,  $\beta$ -strands, and  
536 loops. One calcium ion is represented by a sphere. The loop between  $\beta$ -strands  $\beta_2$  and  $\beta_3$ , as well as  
537 the loop between  $\beta$ -strand  $\beta_4$  and  $\alpha$ -helix  $\alpha_3$  were partially not built due to a lack of density and  
538 these disordered residues are modeled as dashed lines. (b) Native PAGE control of the composition  
539 of the crystal generated from pure  $\alpha$ -La  $A_1$ . Mainly mono-deamidated isoform  $A_2$  was generated  
540 during the crystallogenesis.

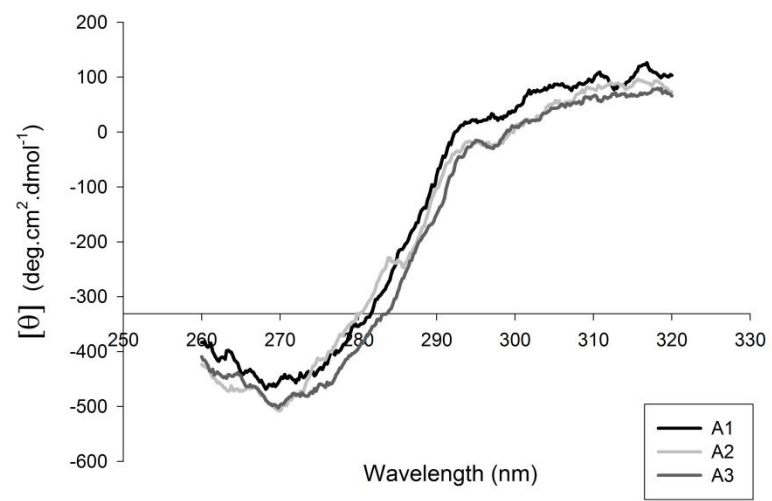
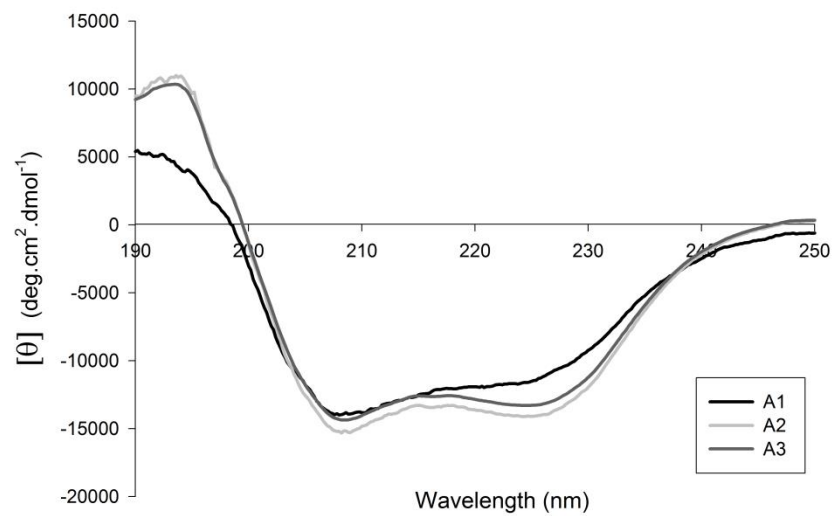
541 **Fig. 4.** DSC thermograms of native ( $A_1$ ), mono-deamidated ( $A_2$ ), and di-deamidated ( $A_3$ )  $\alpha$ -La. Cp,  
542 heat capacity.

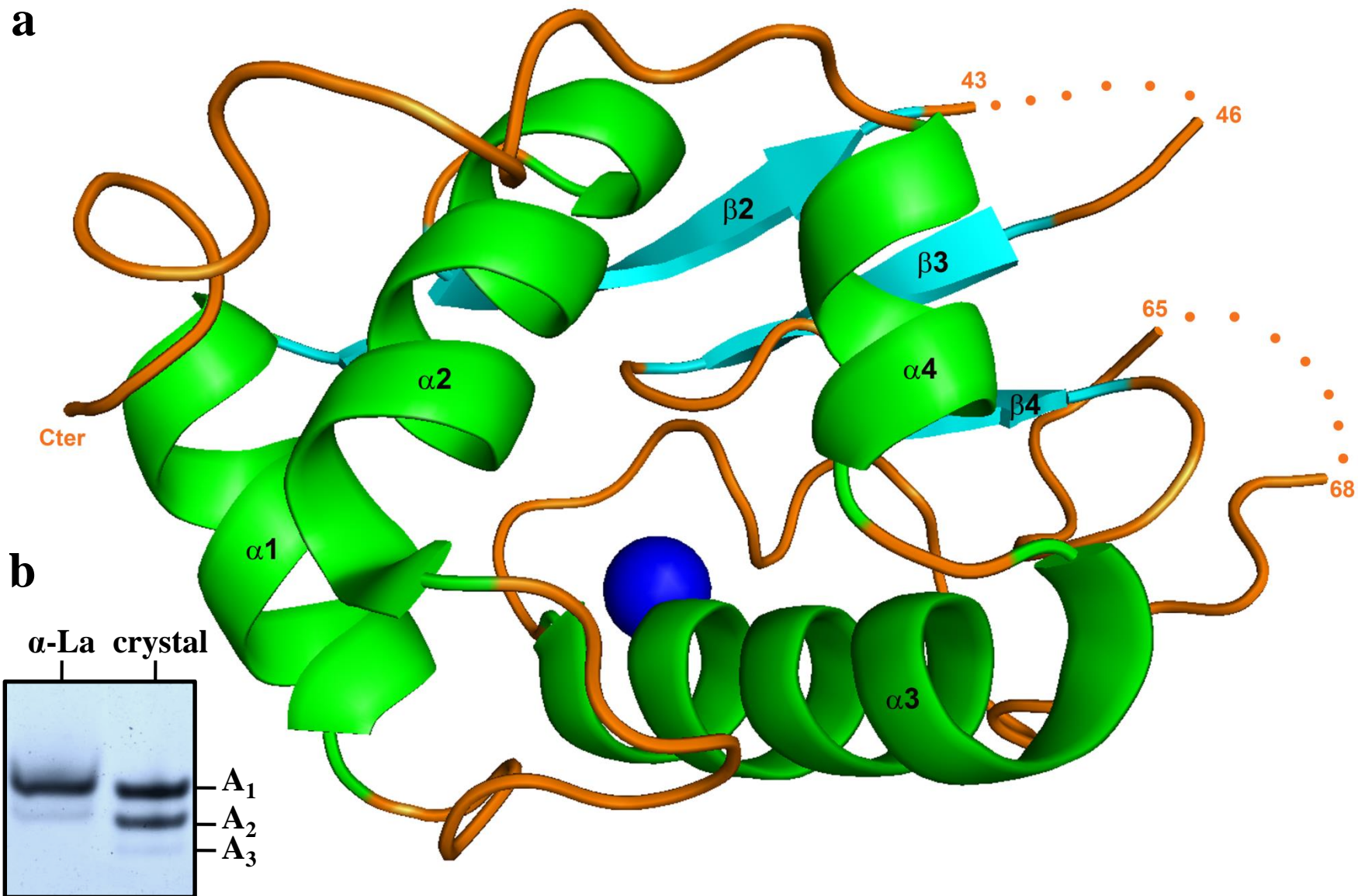
543 **Fig. 5.** Reversed-phase HPLC analysis of native ( $A_1$ ), mono-deamidated ( $A_2$ ), and di-deamidated  
544 ( $A_3$ )  $\alpha$ -La hydrolyzed by thermolysin, in comparison to bovine  $\alpha$ -La hydrolysis. Proteolysis  
545 conditions: Enzyme-to-substrate ratio 1/80, pH 7.2, incubation at 37 °C for 30 to 180 min. Abs<sub>215</sub>,  
546 absorbance at 215 nm.

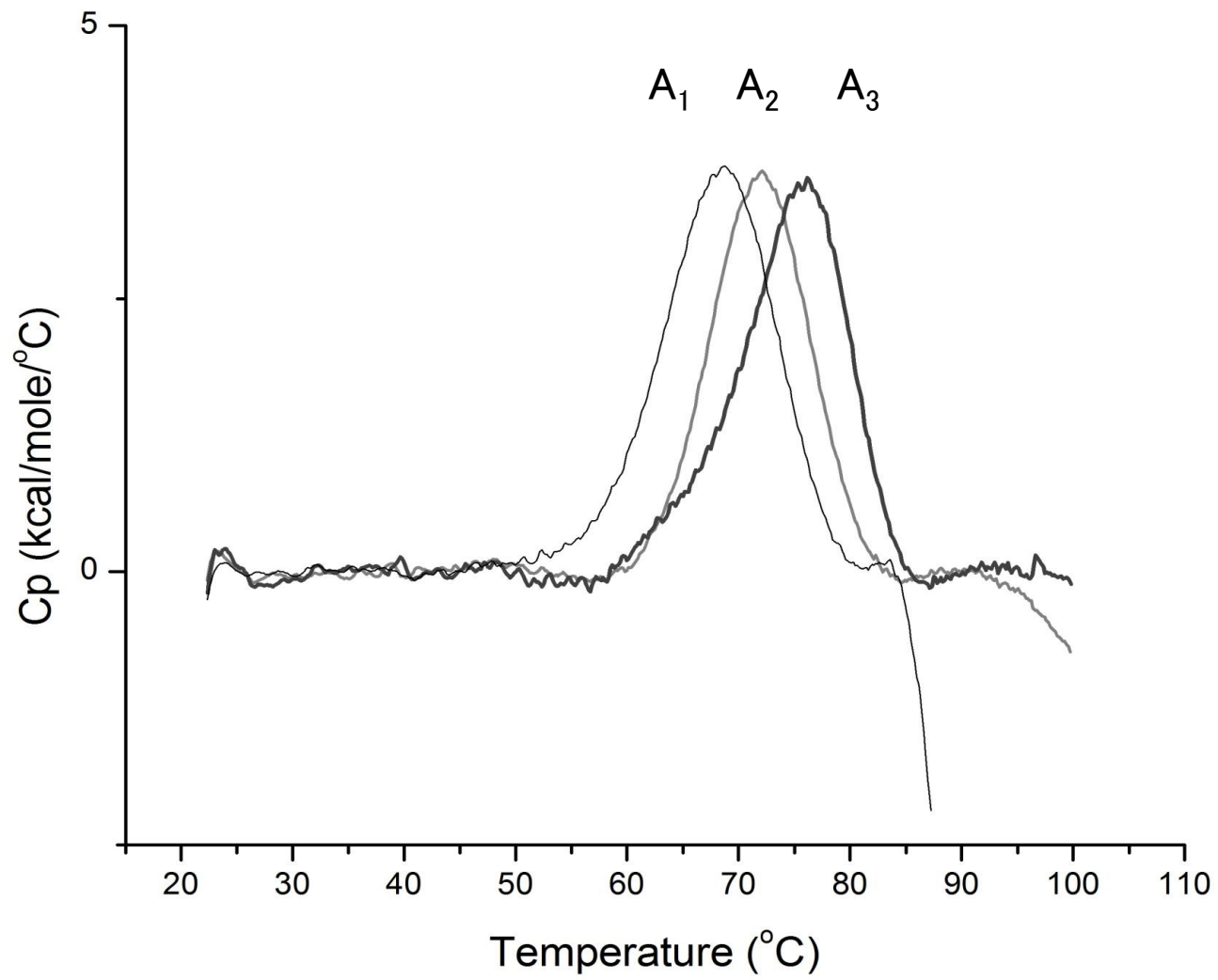
547











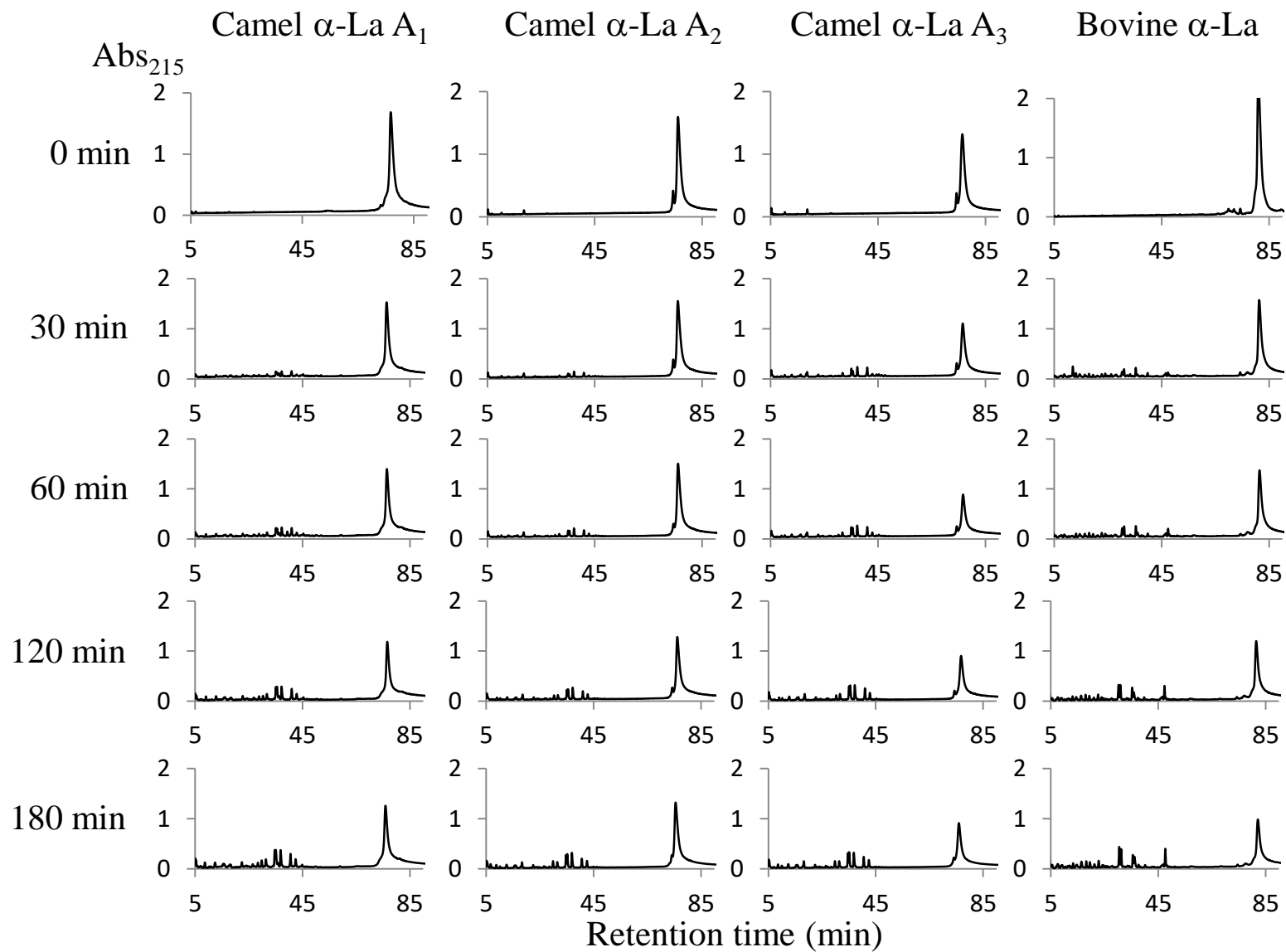


**Table 1**

Secondary structure content and thermodynamic parameters of the native and deamidated isoforms of camel  $\alpha$ -lactalbumin ( $\alpha$ -La) as a comparison to reported values for camel and bovine holo- $\alpha$ -lactalbumins.

Reference	Protein	$\alpha$ -Helix (%)	$\beta$ -Strand (%)	$\beta$ -Turn (%)	Random coil (%)	Tm (°C)	$\Delta H_{cal}$ (kJ/mol)
Present study	$\alpha$ -La A <sub>1</sub>	37.0	15.1	16.4	27.8	68.7 $\pm$ 0.1**	242 $\pm$ 13
	$\alpha$ -La A <sub>2</sub>	42.1	12.9	15.4	25.4	71.9 $\pm$ 0.9**	231 $\pm$ 21
	$\alpha$ -La A <sub>3</sub>	39.7	13.9	15.8	27.0	74.9 $\pm$ 0.2**	229 $\pm$ 19
Atri et al. (2010)	Camel $\alpha$ -La	43.1	13.6	15.8	28.3	71.7 $\pm$ 0.1	222 $\pm$ 38
	Bovine $\alpha$ -La	42.2	13.3	15.6	27.9	67.4 $\pm$ 2.4	243 $\pm$ 4

\*\* :  $p < 0.01$ ; the data are expressed as mean  $\pm$  SD, n = 3